Geophys. J. Int. (1997) **131**, 293–309

Time-domain electromagnetic migration in the solution of inverse problems

Michael S. Zhdanov and Oleg Portniaguine

University of Utah, Department of Geology and Geophysics, Salt Lake City, UT 84112, *USA. E-mail: mzhdanov@mines.utah.edu*

Accepted 1997 June 2. Received 1997 April 4; in original form 1996 July 8

SUMMARY

Time-domain electromagnetic (TDEM) migration is based on downward extrapolation of the observed field in reverse time. In fact, the migrated EM field is the solution of the boundary-value problem for the adjoint Maxwell's equations. The important question is how this imaging technique can be related to the solution of the geoelectrical inverse problem. In this paper we introduce a new formulation of the inverse problem, based on the minimization of the residual-field energy flow through the surface or profile of observations. We demonstrate that TDEM migration can be interpreted as the first step in the solution of this specially formulated TDEM inverse problem. However, in many practical situations this first step produces a very efficient approximation to the geoelectrical model, which makes electromagnetic migration so attractive for practical applications. We demonstrate the effectiveness of this approach in inverting synthetic and practical TDEM data.

Key words: electromagnetic inversion, inverse problem, migration.

1 INTRODUCTION

Time-domain electromagnetic (EM) migration is based on downward extrapolation of the residual field in reverse time. The basic principles of EM migration have been formulated in Zhdanov (1988), Zhdanov, Matusevich & Frenkel (1988), Zhdanov & Keller (1994) and Zhdanov, Traynin & Booker (1996). EM migration has important features in common with seismic migration (Zhdanov *et al.* 1988; Claerbout 1985) but differs in that for geoelectric problems EM migration is carried out on the basis of Maxwell's equations, while in the seismic case it is based on the wave equation. We have introduced time-domain EM migration as the solution of the boundary-value problem in the lower half-space for the adjoint Maxwell's equations, in which the boundary values of the migration field on the earth's surface are determined by the observed EM field.

In the paper by Zhdanov, Traynin & Portniaguine (1995) a technique for transforming the EM migration fields and their different components into resistivity images of the vertical cross-section was developed. However, the question still remains open how this imaging technique can be related to the solution of the geoelectrical inverse problem. Meanwhile, Tarantola (1987) demonstrated that seismic-wave migration, which was the prototype for EM migration, can be treated exactly as the first iteration in some general wave-inversion scheme. In the paper by Wang *et al.* (1994) this analogy was extended to the case of the diffusive transient EM field.

In this paper we formulate and prove an important new result: *EM migration, as the solution of the boundary-value problem for the adjoint Maxwell's equation, can be clearly associated with the inverse-problem solution.* We introduce the residual EM field as the difference between the simulated EM field for some given (background) geoelectrical model and the actual EM field. The EM energy flow of the residual field through the surface of observations can be treated as a functional of the anomalous conductivity distribution in the model. The analysis shows that the gradient of the residual-field energy-flow functional with respect to the perturbation of the model conductivity is equal to the vector cross-correlation function between the incident (background) field and the migrated residual field, calculated as the solution of the boundary-value problem for the adjoint Maxwell's equation.

This result clearly leads to a construction of the rigorous method of solving the inverse EM problem, based on iterative EM migration in the time domain, and a gradient (or conjugate gradient) search for the optimal geoelectrical model. However, the authors have found that in the framework of this method even the first iteration, based on the migration of the residual field, generates a reasonable geoelectrical image of the subsurface structure. We call the anomalous conductivity, calculated on the first iteration, the *migration apparent conductivity.* We obtain a simple integral relationship between the migration apparent conductivity and actual anomalous conductivity, similar to the relationship established in the time domain for the inversion method based on the back-propagated TEM field (M. Oristaglio, personal communication, 1996). It describes the space filtering of the actual conductivity with the Green's-type function. We believe that this relationship will

help to improve the migration imaging conditions because it opens the way for straightforward transformation of the migration apparent conductivity into the real conductivity. We compare these new imaging conditions with the traditional one, obtained for simplified geoelectrical models of the subsurface structures (Zhdanov *et al.* 1995).

In summary, in this paper we demonstrate that EM migration imaging can also be considered as the initial step in the general EM inversion procedure, based on the minimization of the residual-field energy flow through the surface of observations. This similarity facilitates a better understanding of the mathematical and physical background of EM migration and, at the same time, helps in developing new geoelectrical imaging tools.

2 TIME-DOMAIN ELECTROMAGNETIC MIGRATION AS THE SOLUTION OF THE BOUNDARY-VALUE PROBLEM

Let us formulate a general time-domain EM inverse problem. Consider a 3-D geoelectrical model consisting of a homogeneous atmosphere and an inhomogeneous earth with the conductivity $\sigma(\mathbf{r})=\sigma_b(\mathbf{r})+\sigma_a(\mathbf{r})$, where $\sigma_b(\mathbf{r})$ is some background (normal) distribution of the conductivity, and $\sigma_a(\mathbf{r})$ is the anomalous conductivity, which is not equal to zero only within some domain D. We will denote the surface of the earth by Σ. We will confine ourselves to the consideration of non-magnetic media and hence assume that $\mu=\mu_0=4\pi\times10^{-7}$ H m^{-1}, where μ_0 is the free-space magnetic permeability. The EM field in this model is generated by an arbitrarily located source with the current density $\mathbf{j}^e$. Receivers are located on the surface of the earth. We assume also that the EM field is varying in time relatively slowly, so that in the equations for this field the second derivative with respect to the time $\partial^2/\partial t^2$ can be discarded. In other words, we consider the so-called quasi-stationary model of the EM field (without displacement currents) (Zhdanov 1988).

We can represent the total EM field observed in this model as the sum of the background (normal) field $\{\mathbf{E}^b,\mathbf{H}^b\}$ generated by the given source in the model with the background conductivity distribution, and an anomalous field $\{\mathbf{E}^a,\mathbf{H}^a\}$, which is due to an inhomogeneity $\sigma_a(\mathbf{r})$:

$$\mathbf{E}=\mathbf{E}^b+\mathbf{E}^a,\qquad \mathbf{H}=\mathbf{H}^b+\mathbf{H}^a. \tag{1}$$

The total EM field satisfies Maxwell's equations:

$$\nabla\times\mathbf{H}=(\sigma_b+\sigma_a)\mathbf{E}+\mathbf{j}^e,$$
$$\nabla\times\mathbf{E}=-\mu\frac{\partial\mathbf{H}}{\partial t}, \tag{2}$$

while the anomalous field satisfies the equations:

$$\nabla\times\mathbf{H}^a=\sigma_b\mathbf{E}^a+\sigma_a(\mathbf{E}^b+\mathbf{E}^a),$$
$$\nabla\times\mathbf{E}^a=-\mu\frac{\partial\mathbf{H}^a}{\partial t}. \tag{3}$$

The general EM inverse problem can be formulated as follows. We are given the observed total EM field on the surface of the earth and the background (normal) distribution of the conductivity $\sigma_b(\mathbf{r})$. The problem is to determine the anomalous conductivity $\sigma_a(\mathbf{r})$.

In this section we introduce first the migrated anomalous EM field and show how it can be calculated from the anomalous field. In the following sections we will demonstrate the connections between the migrated EM fields and the solution of the EM inverse problem.

It is known (Zhdanov 1988) that the anomalous EM field in this model can be expressed as an integral over the anomalous domain D of the product of the corresponding Green's tensors and excessive currents $\sigma_a(\mathbf{E}^b+\mathbf{E}^a)$:

$$\mathbf{E}^a(\mathbf{r},t)=\int_{-\infty}^{\infty}\iiint_D\hat{G}_E^b(\mathbf{r},t|\mathbf{r}',t')\cdot\sigma_a(\mathbf{r}')\cdot[\mathbf{E}^b(\mathbf{r}',t')+\mathbf{E}^a(\mathbf{r}',t')]\,dv'dt', \tag{4}$$

and

$$\mathbf{H}^a(\mathbf{r},t)=\int_{-\infty}^{\infty}\iiint_D\hat{G}_H^b(\mathbf{r},t|\mathbf{r}',t')\cdot\sigma_a(\mathbf{r}')\cdot[\mathbf{E}^b(\mathbf{r}',t')+\mathbf{E}^a(\mathbf{r}',t')]\,dv'dt', \tag{5}$$

where $\hat{G}_E^b$ and $\hat{G}_H^b$ are the electric and magnetic Green's tensors for the background conductivity $\sigma_b(\mathbf{r})$, whose vector components relate the electric and magnetic fields excited at the point $\mathbf{r}$ by an electric dipole source of unit intensity located at the point $\mathbf{r}'$ of the domain D. The basic equations for Green's tensors and their properties are briefly summarized in Appendix A.

A general definition of the EM migration field has been given in the Zhdanov (1988). According to this definition, the migration field is the solution of the boundary-value problem for the adjoint Maxwell's equations. For example, we can introduce the migration anomalous field $\mathbf{E}^{am}$ and $\mathbf{H}^{am}$, as the field, determined in reverse time $\tau=-t$, whose tangential components are equal to the anomalous field in the reverse time at the surface of the earth, Σ:

$$\mathbf{n}\times\mathbf{E}^{am}(\mathbf{r},\tau)=\mathbf{n}\times\mathbf{E}^a(\mathbf{r},-\tau),$$
$$\mathbf{n}\times\mathbf{H}^{am}(\mathbf{r},\tau)=\mathbf{n}\times\mathbf{H}^a(\mathbf{r},-\tau),\qquad \mathbf{r}\in\Sigma, \tag{6}$$

where $\mathbf{n}$ is the unit vector of the normal to Σ directed into the upper half-space and satisfying Maxwell's equations in reverse time within the earth with a background conductivity σ_b:

$$\nabla\times\mathbf{H}^{am}=\sigma_b\mathbf{E}^{am},$$
$$\nabla\times\mathbf{E}^{am}=-\mu\frac{\partial\mathbf{H}^{am}}{\partial\tau}. \tag{7}$$

From (7) we can obtain the separate equation for the migrated anomalous electric field:

$$\nabla\times\nabla\times\mathbf{E}^{am}=-\mu\sigma_b\frac{\partial\mathbf{E}^{am}}{\partial\tau}. \tag{8}$$

Therefore, in reverse time τ, the electric migrated field satisfies the ordinary vector diffusion equation. However, in direct time $t=-\tau$ the migrated anomalous electric field satisfies the equations adjoint to (8):

$$\nabla\times\nabla\times\mathbf{E}^{am}=\mu\sigma_b\frac{\partial\mathbf{E}^{am}}{\partial t}. \tag{9}$$

While the ordinary diffusion equation describes the development of the process of EM field propagation in an increasing time from the source to the receiver, eq. (9) reflects the same process in the reverse order, that is from the final distribution of the field at the receivers to its initial distribution at the sources. Eq. (9) can thus be called, following Wang *et al.*

(1994), the *vector concentration equation*. As a result, the EM migration field can be treated as the field converging into the sources of the anomalous field, which actually coincide with the geoelectrical inhomogeneities.

The solution of the boundary value problem (6) and (7) for the concentration equation can be obtained on the basis of Green tensor formula (B3) (see Appendix B). We assume that the volume D is bounded by the surface S, which is composed of the surface of the earth Σ and an infinitely large hemisphere in the lower half-space. Since the electromagnetic field satisfies the radiation conditions, that is the functions $\mathbf{E}^{am}$ and $\mathbf{H}^{am}$ vanish exponentially at infinity, the surface integral over the infinitely large hemisphere tends to zero. If we substitute, in formula (B3) from Appendix B, the field $\mathbf{F}$ with the migrated field $\mathbf{E}^{am}(\mathbf{r}, \tau)$, and the tensor $\hat{P}$ with the adjoint Green's tensor $\hat{G}_E^{b+}(\mathbf{r}, \tau|\mathbf{r}', \tau')$, determined in Appendix A, we obtain the following:

$$\begin{aligned}\iiint_D \{[\nabla \times \nabla \times \mathbf{E}^{am}(\mathbf{r}, \tau)] \cdot \hat{G}_E^{b+}(\mathbf{r}, \tau|\mathbf{r}', \tau') \\ - \mathbf{E}^{am}(\mathbf{r}, \tau) \cdot [\nabla \times \nabla \times \hat{G}_E^{b+}(\mathbf{r}, \tau|\mathbf{r}', \tau')]\}\, dv \\ = \iint_\Sigma \mathbf{n} \cdot \{\mathbf{E}^{am}(\mathbf{r}, \tau) \times [\nabla \times \hat{G}_E^{b+}(\mathbf{r}, \tau|\mathbf{r}', \tau')] \\ + [\nabla \times \mathbf{E}^{am}(\mathbf{r}, \tau)] \times \hat{G}_E^{b+}(\mathbf{r}, \tau|\mathbf{r}', \tau')\}\, ds. \qquad (10)\end{aligned}$$

Integrating the left-hand and right-hand sides of expression (10) over time τ and taking into account eqs (8) and (A5), after some algebraic calculations we obtain

$$\begin{aligned}\mathbf{E}^{am}(\mathbf{r}', \tau') = \int_{-\infty}^{+\infty} \iint_\Sigma \mathbf{n} \cdot \{\mathbf{E}^{am}(\mathbf{r}, \tau) \times [\hat{G}_H^{b+}(\mathbf{r}, \tau|\mathbf{r}', \tau')] \\ - \mathbf{H}^{am}(\mathbf{r}, \tau) \times \hat{G}_E^{b+}(\mathbf{r}, \tau|\mathbf{r}', \tau')\}\, ds d\tau. \qquad (11)\end{aligned}$$

Returning from the reverse time, τ, to the ordinary time, $t = -\tau$, and taking into account the reciprocal relations (A3) and (A4) from Appendix A and boundary conditions (6) for the migration field, we can finally write

$$\begin{aligned}\mathbf{E}^{am}(\mathbf{r}', -t') = \int_{-\infty}^{+\infty} \iint_\Sigma \mathbf{n} \cdot \{\mathbf{E}^{a}(\mathbf{r}, t) \times [\hat{G}_H^{b}(\mathbf{r}, t|\mathbf{r}', t')] \\ - \mathbf{H}^{a}(\mathbf{r}, t) \times \hat{G}_E^{b}(\mathbf{r}, t|\mathbf{r}', t')\}\, ds dt. \qquad (12)\end{aligned}$$

Integral formula (12) describes the solution of the concentration equation for the migrated anomalous electric field. The corresponding integral representation for the migrated anomalous magnetic field can be obtained from (12) using the second Maxwell's equation. These integral transformations describe the conversion of the anomalous EM field, generated by the excess currents in the geoelectrical inhomogeneties and diverging in real media, into the migration field, converging to the corresponding inhomogeneties. This process is actually equivalent to the field transformation in ordinary optical holography (Zhdanov 1988). In the next sections we will show how this converging field can be used for the solution of the EM inverse problem.

3 MINIMIZATION OF THE RESIDUAL EM-FIELD ENERGY FLOW

The energy flow of the electromagnetic field can be calculated using the Poynting vector $\mathbf{P}$ (Stratton 1941), introduced by the following formula:

$$\mathbf{P} = \mathbf{E} \times \mathbf{H}.$$

The Poynting vector $\mathbf{P}$ may be interpreted as the intensity of EM energy flow at a given point, that is the energy per second crossing a unit area whose normal is oriented in the direction of the vector $\mathbf{E} \times \mathbf{H}$. For example, the total energy flow of the anomalous EM field through the surface of the earth Σ is equal to

$$Q = \iint_\Sigma \mathbf{P} \cdot \mathbf{n} ds = \iint_\Sigma (\mathbf{E} \times \mathbf{H}) \cdot \mathbf{n} ds,$$

where $\mathbf{n}$ is the unit vector of the normal to the surface Σ directed to the upper half-space (assuming that the sources of the anomalous field are located in the lower half-space).

We denote the observed EM field as $\{\mathbf{E}_{obs}, \mathbf{H}_{obs}\}$. The theoretical EM field, calculated for the given geoelectrical model $\sigma(\mathbf{r}) = \sigma_b(\mathbf{r}) + \sigma_a(\mathbf{r})$, we denote as $\{\mathbf{E}_{pr}, \mathbf{H}_{pr}\}$ (predicted field). According to eq. (1),

$$\begin{aligned}\mathbf{E}_{obs} = \mathbf{E}^b + \mathbf{E}^a_{obs}, \qquad \mathbf{H}_{obs} = \mathbf{H}^b + \mathbf{H}^a_{obs}, \\ \mathbf{E}_{pr} = \mathbf{E}^b + \mathbf{E}^a_{pr}, \qquad \mathbf{H}_{pr} = \mathbf{H}^b + \mathbf{H}^a_{pr}. \qquad (13)\end{aligned}$$

Now, we determine the residual field $\{\mathbf{E}^\Delta, \mathbf{H}^\Delta\}$ as the difference between the observed and predicted fields:

$$\begin{aligned}\mathbf{E}^\Delta(\mathbf{r}, t) = \mathbf{E}_{obs}(\mathbf{r}, t) - \mathbf{E}_{pr}(\mathbf{r}, t) = \mathbf{E}^a_{obs}(\mathbf{r}, t) - \mathbf{E}^a_{pr}(\mathbf{r}, t), \\ \mathbf{H}^\Delta(\mathbf{r}, t) = \mathbf{H}_{obs}(\mathbf{r}, t) - \mathbf{H}_{pr}(\mathbf{r}, t) = \mathbf{H}^a_{obs}(\mathbf{r}, t) - \mathbf{H}^a_{pr}(\mathbf{r}, t). \qquad (14)\end{aligned}$$

We can introduce the energy flow of the residual field through the surface of the earth:

$$Q^\Delta = \iint_\Sigma [\mathbf{E}^\Delta(\mathbf{r}, t) \times \mathbf{H}^\Delta(\mathbf{r}, t)] \mathbf{n} ds.$$

Pankratov, Avdeev & Kuvshinov (1995) have proved an important theorem, according to which the energy flow Q^Δ of the residual field is non-negative:

$$Q^\Delta \geq 0. \qquad (15)$$

Based on this theorem we can introduce the measure Φ of the difference between the observed and predicted fields as the energy flow of the residual field through the surface of observations, integrated over the time t:

$$\Phi = \int_{-\infty}^{\infty} \iint_\Sigma [\mathbf{E}^\Delta(\mathbf{r}, t) \times \mathbf{H}^\Delta(\mathbf{r}, t)] \cdot \mathbf{n} ds dt \geq 0.$$

The advantage of this new functional in comparison with the traditional misfit functional is that $\Phi(\sigma_b)$ has a clear physical meaning, that is the residual-field energy flow through the profile of observations. Obviously, the theoretical predicted fields $\mathbf{E}_{pr}(\mathbf{r}, t)$ and $\mathbf{H}_{pr}(\mathbf{r}, t)$ depend on the anomalous conductivity distribution $\sigma_a(x, z)$ in the given geoelectrical model; therefore, Φ can be treated as a functional of the anomalous conductivity model $\Phi = \Phi(\sigma_a)$.

Thus, the EM inversion problem can be reduced to the minimization of the residual-field energy-flow functional,

$$\Phi(\sigma_a) = \min.$$

In the following section we will discuss the solution of this problem.

4 SOLUTION OF THE MINIMUM ENERGY-FLOW PROBLEM

We apply the gradient-type method to the solution of the minimum energy-flow problem, which is based on computing the gradient direction for the misfit functional and decreasing this functional by moving iteratively 'down the hill' (Tarantola 1987) in the space of the inverse-problem solutions.

Following the conventional ideas of the steepest-descent method, we calculate the first variation of the energy-flow functional in order to find the gradient direction:

$$\delta\Phi = -\int_{-\infty}^{\infty}\iint_{\Sigma}\mathbf{n}\cdot[\mathbf{E}^{\Delta}(\mathbf{r},t)\times\delta\mathbf{H}^{a}_{pr}(\mathbf{r},t) - \mathbf{H}^{\Delta}(\mathbf{r},t)\times\delta\mathbf{E}^{a}_{pr}(\mathbf{r},t)]\,ds\,dt. \tag{16}$$

The perturbations of anomalous electric and magnetic fields can be expressed through the perturbation of the anomalous conductivity $\delta\sigma_a$ using the integral formulae similar to eq. (4) (Zjhdanov & Keller 1994; Wang *et al.* 1994):

$$\delta\mathbf{E}^{a}_{pr}(\mathbf{r},t) = \int_{-\infty}^{\infty}\iiint_{D}\hat{G}^{b}_{E}(\mathbf{r},t|\mathbf{r}',t')\cdot\delta\sigma_a(\mathbf{r}')\cdot[\mathbf{E}^{b}(\mathbf{r}',t')+\mathbf{E}^{a}_{pr}(\mathbf{r}',t')]\,dv'dt',$$

$$\delta\mathbf{H}^{a}_{pr}(\mathbf{r},t) = \int_{-\infty}^{\infty}\iiint_{D}\hat{G}^{b}_{H}(\mathbf{r},t|\mathbf{r}',t')\cdot\delta\sigma_a(\mathbf{r}')\cdot[\mathbf{E}^{b}(\mathbf{r}',t')+\mathbf{E}^{a}_{pr}(\mathbf{r}',t')]\,dv'dt'.$$

Substituting the last equations into (16) we find

$$\delta\Phi = -\iiint_{D}\delta\sigma_a(\mathbf{r}')\int_{-\infty}^{\infty}\int_{-\infty}^{\infty}\iint_{\Sigma}\mathbf{n}\cdot\{\mathbf{E}^{\Delta}(\mathbf{r},t)\times\hat{G}^{b}_{H}(\mathbf{r},t|\mathbf{r}',t') - \mathbf{H}^{\Delta}(\mathbf{r},t)\times\hat{G}^{b}_{E}(\mathbf{r},t|\mathbf{r}',t')\,ds\}\,dt\cdot[\mathbf{E}^{b}(\mathbf{r}',t')+\mathbf{E}^{a}_{pr}(\mathbf{r}',t')]\,dt'dv'. \tag{17}$$

According to eq. (12) the integral over the earth's surface can be treated as the migration of the residual field:

$$\int_{-\infty}^{+\infty}\iint_{\Sigma}\mathbf{n}\cdot\{\mathbf{E}^{\Delta}(\mathbf{r},t)\times\hat{G}^{b}_{H}(\mathbf{r},t|\mathbf{r}',t') - \mathbf{H}^{\Delta}(\mathbf{r},t)\times\hat{G}^{b}_{E}(\mathbf{r},t|\mathbf{r}',t')\}\,ds\,dt = \mathbf{E}^{\Delta m}(\mathbf{r}',-t'). \tag{18}$$

Substituting eq. (18) into (17), and taking into account (13), we obtain

$$\delta\Phi(\sigma_a,\delta\sigma_a) = -\iiint_{D}\delta\sigma_a(\mathbf{r})\int_{-\infty}^{\infty}\mathbf{E}^{\Delta m}(\mathbf{r},-t)\cdot\mathbf{E}_{pr}(\mathbf{r},t)\,dt\,dv, \tag{19}$$

where we have omitted the primes on $\mathbf{r}$ and t to simplify the formula.

We have to find a perturbation of the anomalous conductivity $\delta\sigma_a(\mathbf{r})$ that will reduce the energy-flow functional. In this case we go 'down the hill' in the space of the inverse-problem solutions. The obvious choice is

$$\delta\sigma_a(\mathbf{r}) = k_0\int_{-\infty}^{\infty}\mathbf{E}^{\Delta m}(\mathbf{r},-t)\cdot\mathbf{E}_{pr}(\mathbf{r},t)\,dt, \tag{20}$$

where $k_0 > 0$ is the length of a step. In this case the first variation of the energy-flow functional is negative:

$$\delta\Phi(\sigma_a,\delta\sigma_a) = -k_0\iiint_{D}[\delta\sigma_a(\mathbf{r})]^2\,dv < 0.$$

Let us select the initial conductivity distribution model to be equal to the background conductivity, that is the initial anomalous conductivity is equal to zero:

$$\sigma_{a(0)}(\mathbf{r}) = 0. \tag{21}$$

Then the corresponding anomalous part of the predicted field $\mathbf{E}^{a(0)}_{pr}(\mathbf{r},t)$ is also equal to zero:

$$\mathbf{E}^{a(0)}_{pr}(\mathbf{r},t) = 0, \tag{22}$$

and

$$\mathbf{E}^{(0)}_{pr}(\mathbf{r},t) = \mathbf{E}^{b}(\mathbf{r},t). \tag{23}$$

The first iteration, according to eqs (20), (21) and (23), is given by the formula

$$\sigma_{a(1)}(\mathbf{r}) = \sigma_{a(0)}(\mathbf{r}) - k_0 l_0(\mathbf{r}) = -k l_0(\mathbf{r}), \tag{24}$$

where $l_0(\mathbf{r})$ is the gradient direction (with the minus sign):

$$l_0(\mathbf{r}) = -\int_{-\infty}^{\infty}\mathbf{E}^{\Delta m}(\mathbf{r},-t)\cdot\mathbf{E}^{(0)}_{pr}(\mathbf{r},t)\,dt. \tag{25}$$

The optimal length of the step k_0 can be determined by a line search for the minimum (Fletcher 1987) of the functional

$$\Phi[\sigma_b(x,z) - k_0 l_0(x,z)] = \Phi(k_0) = \min,$$

with respect to k_0. Appendix C contains the detailed derivation of the corresponding expression for k_0.

Eq. (24) describes the migration imaging condition for determining the anomalous conductivity distribution from the migrated residual electric field. Obviously, the corresponding value $\sigma_{a(1)}(\mathbf{r})$ provides only a first approximation to the real anomalous conductivity. To improve the resolution of the method, we can repeat the same procedure, which results in an iterative time-domain migration. The general iterative process can be described by the formula

$$\sigma_{a(n+1)}(\mathbf{r}) = \sigma_{a(n)}(\mathbf{r}) + \delta\sigma_{(n)}(\mathbf{r}) = \sigma_{a(n)}(\mathbf{r}) - k_n l_n(\mathbf{r}), \qquad \mathbf{r}\in D.$$

The gradient direction on the nth iteration, $l_n(\mathbf{r})$, can be calculated by the formula, analogous to (25),

$$l_n(\mathbf{r}) = -\int_{-\infty}^{\infty}\mathbf{E}^{\Delta_n m}(\mathbf{r},-t)\cdot\mathbf{E}^{(n)}_{pr}(\mathbf{r},t)\,dt,$$

where $\mathbf{E}^{(n)}_{pr}(\mathbf{r},t)$ is the field calculated by forward modelling for the geoelectrical model with the conductivity distribution $\sigma_{a(n)}(\mathbf{r})$, and $\mathbf{E}^{\Delta_n m}(\mathbf{r},-t)$ is the migration of the residual field $\mathbf{E}^{\Delta_n}$, which is the difference between the observed field and the theoretical predicted field, E^n_y, found on the nth iteration.

It is well known (Zhdanov 1988; Zhdanov & Keller 1994; Zhdanov *et al.* 1995) that the numerical calculation of the migration field is a stable, well-posed problem. However, in the case of iterative migration the complete solution of the inverse problem is an ill-posed problem. To regularize the process of iterative migration we have to introduce a Tikhonov parametric functional (Tikhonov & Arsenin 1977):

$$P^{\alpha}(\sigma) = \Phi(\sigma) + \alpha S(\sigma).$$

The stabilizer $S(\sigma)$ can be determined as an L_2 norm of the difference between the current anomalous conductivity distribution σ_a and some *a priori* model of the anomalous

conductivity $\sigma_{\rm apr}$:

$$S(\sigma)=\|\sigma_{\rm a}-\sigma_{\rm apr}\|^2_{L_2}=\iiint_D[\sigma_{\rm a}(\mathbf{r})-\sigma_{\rm apr}(\mathbf{r})]^2\,dv.$$

In this case the iterative process will be described by the formula

$$\sigma_{{\rm a}(n+1)}(\mathbf{r})=\sigma_{{\rm a}(n)}(\mathbf{r})-k_n^{(\alpha)}l_n^{(\alpha)}(\mathbf{r}), \tag{26}$$

where $l_n^{(\alpha)}(\mathbf{r})$ is the regularized gradient direction on the nth iteration, calculated by the formula

$$l_n^{(\alpha)}(\mathbf{r})=-\int_{-\infty}^{\infty}\mathbf{E}^{\Delta_n{\rm m}}(\mathbf{r},-t)\cdot\mathbf{E}_{\rm pr}^{(n)}(\mathbf{r},t)\,dt+\alpha[\sigma_n(\mathbf{r})-\sigma_{\rm apr}(\mathbf{r})],$$

and the length of the regularized step $k_n^{(\alpha)}$ is calculated using the line search for the minimum of the parametric functional

$$P^{\alpha}(\sigma_{(n)}-k_n^{(\alpha)}l_n^{(\alpha)})=\mathbf{P}^{\alpha}(k_n^{(\alpha)})=\min.$$

Thus, we can describe the developed method of EM inversion as the process of iterative migration. At every step of the iterations we calculate the theoretical EM response for the given geoelectrical model $\sigma_{(n)}(\mathbf{r})$, obtained from the previous step, calculate the residual field between this response and the observed field, and then migrate the residual field. The gradient direction is computed as a vector cross-correlation between the migrated residual field and the theoretical predicted field $\mathbf{E}_{\rm pr}^{(n)}$. Using this gradient direction and the corresponding value of the optimal length of the step $k_n^{(\alpha)}$, we calculate the new geoelectrical model $\sigma_{(n+1)}(\mathbf{r})$ on the basis of expression (26). The iterations are terminated when the functional $\Phi(\sigma)$ reaches the level of the noise energy. The optimal value of the regularization parameter α is selected using conventional principles of regularization theory (Tikhonov & Arsenin 1977).

5 MIGRATION IMAGING AS A SPATIAL FILTERING OF THE ANOMALOUS CONDUCTIVITY

According to eq. (20) we can develop a migration imaging scheme based on the formula

$$\sigma_{\rm ma}(\mathbf{r}')=k_0\int_{-\infty}^{\infty}\mathbf{E}^{\Delta{\rm m}}(\mathbf{r}',-t')\cdot\mathbf{E}^{\rm b}(\mathbf{r}',t')\,dt', \tag{27}$$

where k_0 is determined using eq. (C5) from Appendix C. We will call $\sigma_{\rm ma}(\mathbf{r}')$, determined using expression (27), a migration anomalous conductivity. The important question is how this apparent conductivity is related to the real anomalous conductivity $\sigma_{\rm a}$. The solution of this question can be found directly from formula (27).

Let us express the residual migration field $\mathbf{E}^{\Delta{\rm m}}$ through the observed residual field $\{\mathbf{E}^{\Delta},\mathbf{H}^{\Delta}\}$, using a formula similar to (12):

$$\mathbf{E}^{\Delta{\rm m}}(\mathbf{r}',-t')=\int_{-\infty}^{+\infty}\iint_{\Sigma}\mathbf{n}\{\mathbf{E}^{\Delta}(\mathbf{r},t)\times[\hat{G}_H^{\rm b}(\mathbf{r},t|\mathbf{r}',t')]-\mathbf{H}^{\Delta}(\mathbf{r},t)\times\hat{G}_E^{\rm b}(\mathbf{r},t|\mathbf{r}',t')\}\,dsdt. \tag{28}$$

Substituting (28) into (27), we obtain

$$\sigma_{\rm ma}(\mathbf{r}')=k_0\int_{-\infty}^{\infty}\int_{-\infty}^{+\infty}\iint_{\Sigma}\mathbf{n}\cdot\{\mathbf{E}^{\Delta}(\mathbf{r},t)\times[\hat{G}_H^{\rm b}(\mathbf{r},t|\mathbf{r}',t')]-\mathbf{H}^{\Delta}(\mathbf{r},t)\times\hat{G}_E^{\rm b}(\mathbf{r},t|\mathbf{r}',t')\}\,dsdt\cdot\mathbf{E}^{\rm b}(\mathbf{r}',t')\,dt'. \tag{29}$$

From the other side, according to eqs (14) and (22), the residual field is equal to the observed anomalous field, which can be computed using formulae (4) and (5). For example, for the electric field we have

$$\mathbf{E}^{\Delta}(\mathbf{r},t)=\mathbf{E}^{\rm a}_{\rm obs}(\mathbf{r},t)=\int_{-\infty}^{\infty}\iiint_D\sigma_{\rm a}(\mathbf{r}'')\times[\mathbf{E}^{\rm b}(\mathbf{r}'',t'')+\mathbf{E}^{\rm a}_{\rm obs}(\mathbf{r}'',t'')]\,\tilde{\hat{G}}_E^{\rm b}(\mathbf{r},t|\mathbf{r}'',t'')\,dv''dt'', \tag{30}$$

where we use double-prime notation to distinguish $\mathbf{r}''$ from $\mathbf{r}'$. A similar expression can be obtained for the magnetic field.

Substituting (30) into (29), we find

$$\alpha_{\rm ma}(\mathbf{r}')=k_0\int_{-\infty}^{\infty}\iiint_D\sigma_{\rm a}(\mathbf{r}'')\cdot\int_{-\infty}^{\infty}[\mathbf{E}^{\rm b}(\mathbf{r}'',t'')+\mathbf{E}^{\rm a}_{\rm obs}(\mathbf{r}'',t'')]\cdot\int_{-\infty}^{+\infty}\iint_{\Sigma}\mathbf{n}\cdot\{\tilde{\hat{G}}_E^{\rm b}(\mathbf{r},t|\mathbf{r}'',t'')\times[\hat{G}_H^{\rm b}(\mathbf{r},t|\mathbf{r}',t')]-\tilde{\hat{G}}_H^{\rm b}(\mathbf{r},t|\mathbf{r}'',t'')\times\hat{G}_E^{\rm b}(\mathbf{r},t|\mathbf{r}',t')\}\,dsdt\cdot\mathbf{E}^{\rm b}(\mathbf{r}',t')\,dt'dv''dt''. \tag{31}$$

Applying the Green tensor formula (B4) from Appendix B and executing calculations similar to those of Section 2 for the EM migration field, we obtain

$$\int_{-\infty}^{+\infty}\iint_{\Sigma}\mathbf{n}\cdot\{\tilde{\hat{G}}_H^{\rm b}(\mathbf{r},t|\mathbf{r}'',t'')\times[\hat{G}_H^{\rm b}(\mathbf{r},t|\mathbf{r}',t')]-\tilde{\hat{G}}_H^{\rm b}(\mathbf{r},t|\mathbf{r}'',t'')\times\hat{G}_E^{\rm b}(\mathbf{r},t|\mathbf{r}',t')\}\,dsdt=\hat{G}_E^{\rm bm}(\mathbf{r}',-t'|\mathbf{r}'',t''), \tag{32}$$

where $\hat{G}_E^{\rm bm}$ is the migrated Green's tensor.

Substituting (32) back into eq. (31), we obtain

$$\sigma_{\rm ma}(\mathbf{r}')=k_0\int_{-\infty}^{\infty}\iiint_D\sigma_{\rm a}(\mathbf{r}'')\cdot\int_{-\infty}^{\infty}[\mathbf{E}^{\rm b}(\mathbf{r}'',t'')+\mathbf{E}^{\rm a}_{\rm obs}(\mathbf{r}'',t'')]\cdot\hat{G}_E^{\rm bm}(\mathbf{r}',-t'|\mathbf{r}'',t'')\cdot\mathbf{E}^{\rm b}(\mathbf{r}',t')\,dt'dv''dt''.$$

The last expression can be rewritten in the form:

$$\sigma_{\rm ma}(\mathbf{r}')=\iiint_D\sigma_{\rm a}(\mathbf{r})g(\mathbf{r},\mathbf{r}')\,dv, \tag{33}$$

where

$$g(\mathbf{r},\mathbf{r}')=k_0\int_{-\infty}^{\infty}[\mathbf{E}^{\rm b}(\mathbf{r},t)+\mathbf{E}^{\rm a}_{\rm obs}(\mathbf{r},t)]\cdot\hat{G}_E^{\rm bm}(\mathbf{r}',-t'|\mathbf{r},t)\cdot\mathbf{E}^{\rm b}(\mathbf{r}',t')\,dt'dt. \tag{34}$$

Eq. (33) demonstrates that the migration apparent conductivity $\sigma_{ma}(\mathbf{r}')$ can be treated as the spatial filtering of the real anomalous conductivity with a filter determined by expression (34). This filter is formed by the combination of the Green's tensors, which have local extrema at the point $\mathbf{r}=\mathbf{r}'$. The sharpness of the filter $g(\mathbf{r},\mathbf{r}')$ determines the measure of closeness of the migration apparent conductivity to the real anomalous conductivity.

6 TWO-DIMENSIONAL EM MIGRATION

Consider now a special case of the 2-D E polarized electromagnetic field, excited in a 2-D geoelectrical model by an electrical current of density $\mathbf{j}^{ex} = j^{ex}\mathbf{d}_y$, which is distributed in the domain Q in the upper half-space. We assume that $\{\mathbf{d}_x, \mathbf{d}_y, \mathbf{d}_z\}$ is the orthonormal basis of the Cartesian coordinate system with the origin on the earth's surface, and unit vector $\mathbf{d}_z$ is directed downwards. Within this model, the electromagnetic field can be described by a single function, E_y, satisfying the equation

$$\nabla^2 E_y - \mu_0 \sigma_b \frac{\partial}{\partial t} E_y = \mu_0 \frac{\partial}{\partial t} j^{ex}, \tag{35}$$

and the magnetic field components $\{H_x, H_z\}$ can be expressed

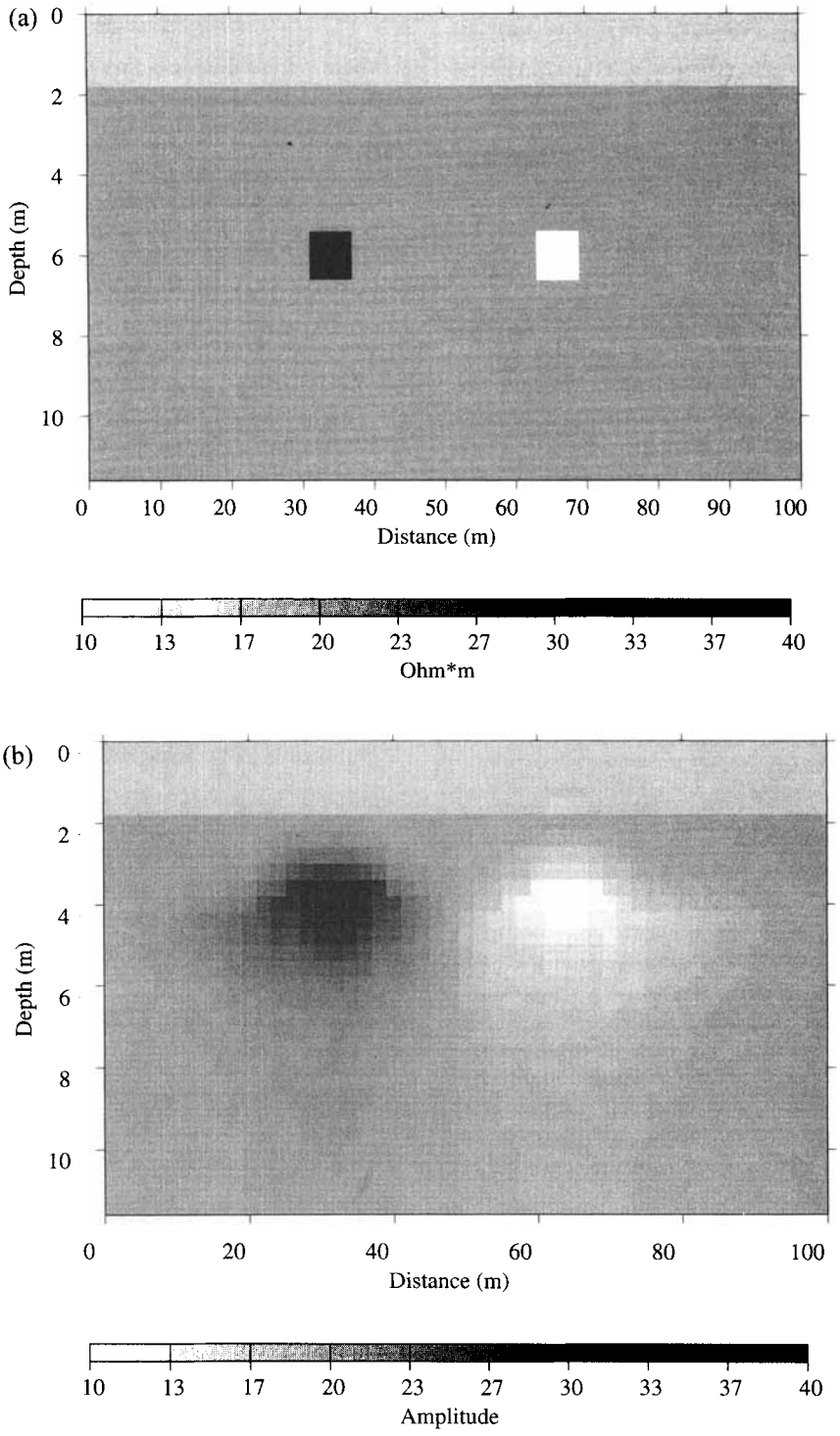

Figure 1. (a) Conductive and resistive bodies in a two-layered host. (b) Migration result for the model with conductive and resistive bodies in a two-layered host.

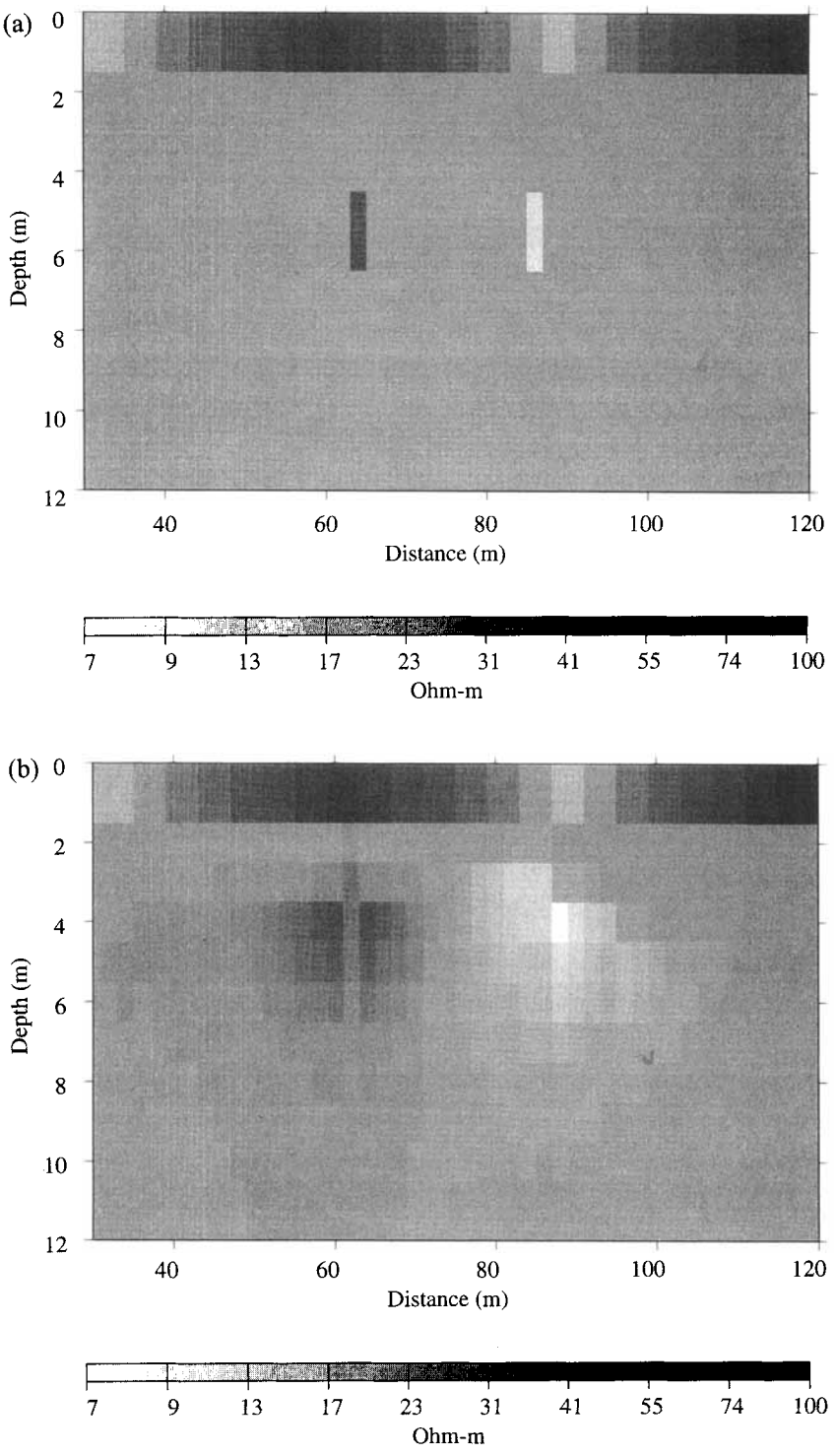

Figure 2. (a) Conductive and resistive bodies in a host with an inhomogeneous surface layer. (b) Migration results for the model with conductive and resistive bodies in a host with an inhomogeneous surface layer.

by the equations

$$\mu_0 \frac{\partial}{\partial t} H_x = \frac{\partial E_y}{\partial z}, \qquad -\mu_0 \frac{\partial}{\partial t} H_z = \frac{\partial E_y}{\partial x}. \tag{36}$$

We can introduce the y-component E_y^{am} of a 2-D migration anomalous field as the field equal to the anomalous electric field in reverse time on the profile L at the surface of the earth:

$$E_y^{\mathrm{am}}(x', z', t) = E_y^{\mathrm{a}}(x', z', -t), \qquad (x', z') \in L, \tag{37}$$

and satisfying the 2-D analogues of eq. (7):

$$\nabla^2 E_y^{\mathrm{am}} + \mu_0 \sigma_{\mathrm{b}} \frac{\partial}{\partial t} E_y^{\mathrm{am}} = 0. \tag{38}$$

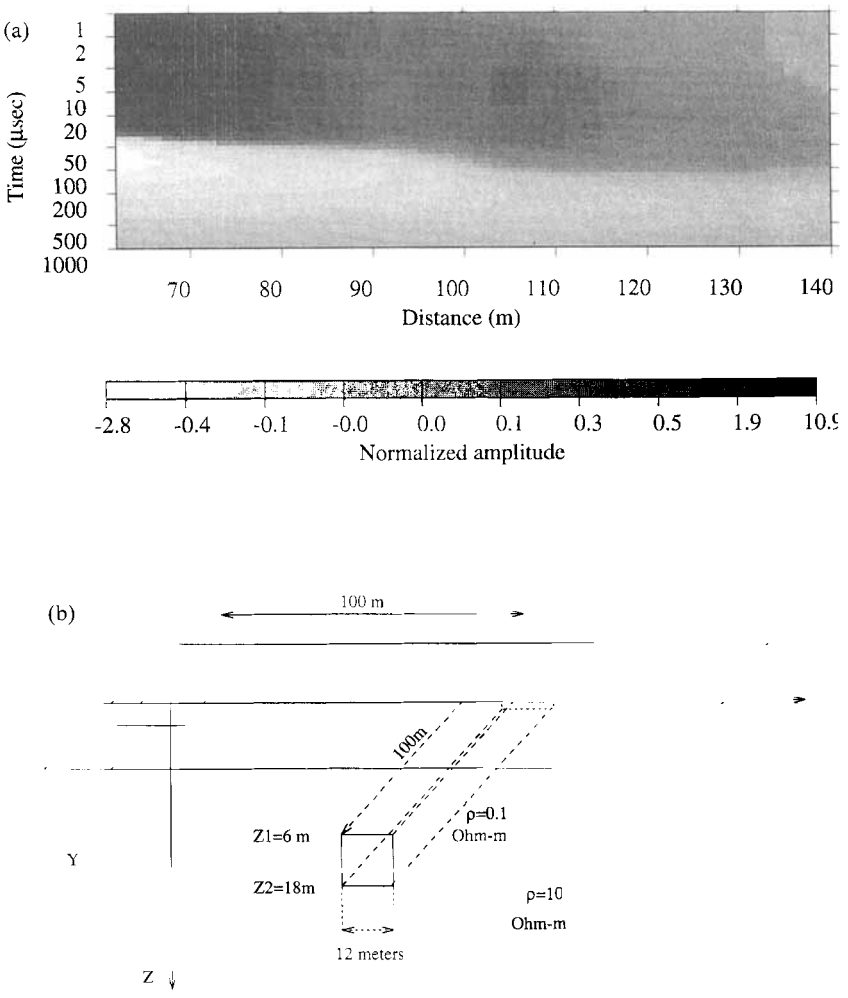

Magnetic components of the 2-D migrated field can be calculated using the second Maxwell's equation:

$$-\mu_0 \frac{\partial}{\partial t} H_x^{am} = \frac{\partial E_y^{am}}{\partial z},$$

$$\mu_0 \frac{\partial}{\partial t} H_z^{am} = \frac{\partial E_y^{am}}{\partial x}.$$

Integral formula (12) for the calculation of the migrated anomalous field E_y^{am} is transformed into the expression

$$E_y^{am}(x', z', -t') = \int_{t'}^{+\infty} \int_L \left[E_y^a(x, z, t) \frac{\partial G^b(x, z, t|x', z', t')}{\partial n} - G^b(x, z, t|x', z', t') \frac{\partial E_y^a(x, z, t)}{\partial n} \right] dl dt, \quad (39)$$

where n is the direction of the normal to the surface of the earth L directed into the upper half-space, and the Green's function $G^b(x, z, t|x', z', t')$ satisfies the equation

$$\nabla^2 G^b - \mu_0 \sigma_b \frac{\partial}{\partial t} G^b = \mu_0 \delta(x - x')(z - z') \frac{\partial \delta(t - t')}{\partial t}.$$

We have also taken into account in eq. (39) that the Green's function $G^b(x, z, t|x', z', t')$ is causal:

$$G^b(x, z, t|x', z', t') \equiv 0, \qquad t \le t'.$$

In the case of the horizontal line L of observations ($z = 0$), expression (39) can be simplified (Zhdanov & Keller 1994) to the following:

$$E_y^{am}(x', z', -t') = -2 \int_{t'}^{+\infty} \int_{-\infty}^{+\infty} E_y^a(x, 0, t) \times \frac{\partial G^b(x, 0, t|x', z', t')}{\partial x} dx dt. \quad (40)$$

The last expression gives us the integral method of calculation of the migrated electric field. We can also transform this formula to find the integral formula for migration of the magnetic field. Indeed, let us differentiate the last equation with respect to x'. After integrating by parts, we find

$$\frac{\partial}{\partial t'} H_z^{am}(x', z', -t') = -2 \int_{t'}^{+\infty} \int_{-\infty}^{+\infty} \frac{\partial}{\partial t} H_z^{am}(x, 0, t) \times \frac{\partial G^b(x, 0, t|x', z', t')}{\partial z} dx dt. \quad (41)$$

Note that typical geophysical EM equipment uses receiver loops for measuring the components of the magnetic field. Therefore, the actual data contain the records of EM induction in the loops, which are proportional to the time derivatives of the magnetic-field variations $(\partial/\partial t)H_z(x, 0, t)$. Therefore,

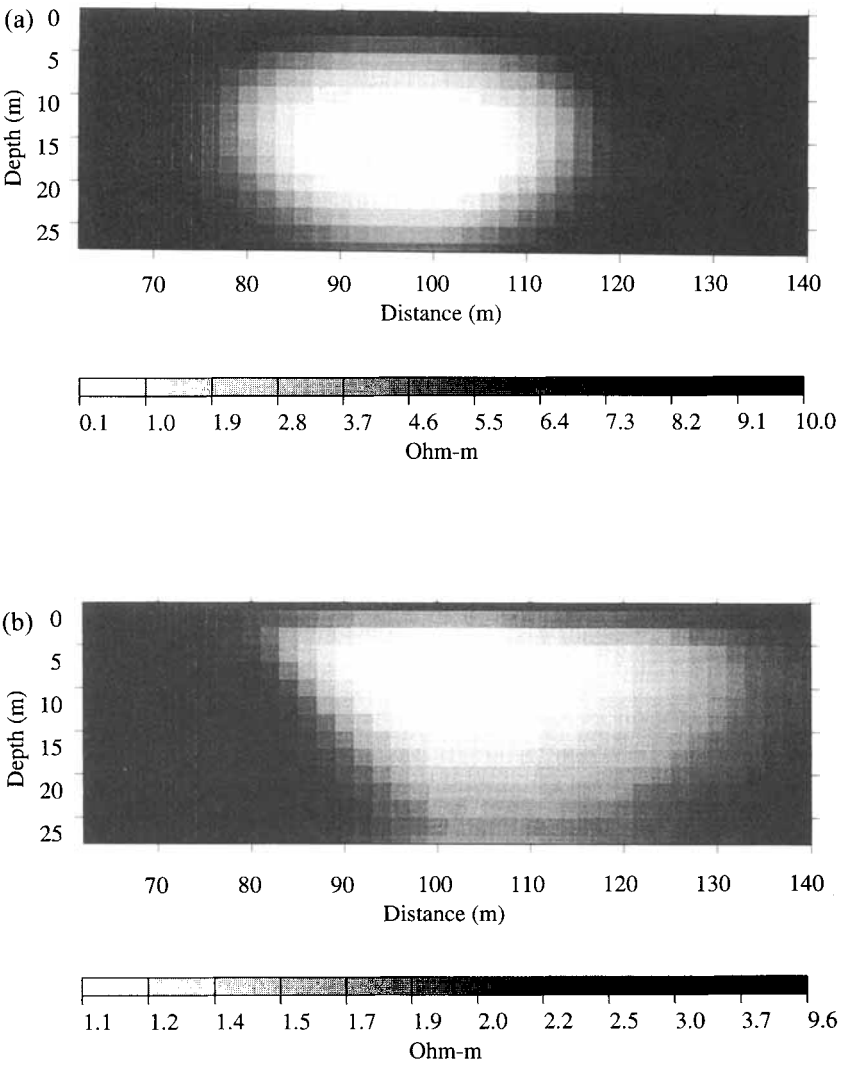

Figure 4. (a) Migration apparent resistivity for a 3-D model with a conductive body computed using approximate imaging conditions. (b) Migration apparent resistivity for a 3-D model with a conductive body computed using the new imaging conditions.

expression (41) solves the problem of the migration of EM induction data. Note that in the 2-D case we can obtain from the migrated field $(\partial/\partial t')H_z^{\mathrm{am}}(x', z', -t')$ the migrated electric field again (Zhdanov *et al.* 1995), using the second Maxwell's equation for the migration field:

$$E_y^{\mathrm{m}}(\tilde{x}, z', -t') = \mu_0 \int_{-\infty}^{\tilde{x}} \frac{\partial}{\partial t'} H_z^{\mathrm{m}}(x', z', -t')\, dx'. \qquad (42)$$

Thus, expressions (40), (41) and (42) solve the problem of the calculation of the migrated electric field on the basis of electric or magnetic observations.

We can now use the 2-D analogue of the imaging condition (27) to calculate the migration anomalous conductivity $\sigma_{\mathrm{ma}}(x', z')$.

7 PRACTICAL ASPECTS OF 2-D MIGRATION IMAGING

Practical realization of the 2-D theory of EM migration, described above, requires the solution of two major problems: (1) the determination of the background conductivity, σ_{b}; and (2) developing the numerical method of EM migration through media with an arbitrary distribution of background conductivity, σ_{b}.

7.1 Determination of the background conductivity σ_{b}

There are several publications dedicated to the development of simple and fast inversion techniques for the processing of transient EM data over inhomogeneous structures (Barnett 1984; Macnae & Lamontagne 1987; Eaton & Hohmann 1989). A majority of these papers were based on equating the transient response, measured at the surface of the Earth, to the EM field of current-filament images of the source. For example, a rapid inversion technique (RIT) developed in Eaton & Hohmann (1989) and based on the earlier work of Macnae & Lamontagne (1987) proved to be an effective method for determining the background resistivity. This approach can be understood well, based on the inspirational work of Nabighian (1979), who described the behaviour of transient currents diffusing into the Earth as a system of 'smoke rings' blown by the transmitting loop into the Earth. The main limitation of the RIT method

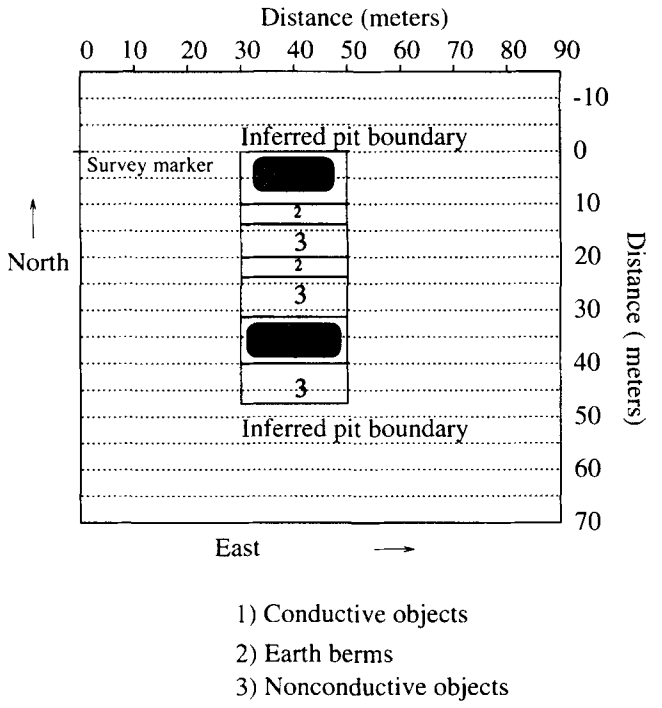

Figure 5. Scheme of object locations in the Cold Test Pit.

is connected to the fact that it is based on a simple 1-D model of underground structures. The key formula for inversion is the expression relating the velocity, V, of 'smoke ring' propagation and the conductivity, σ, in this model:

$$\sigma = f(V).$$

The simple assumption results in a significant averaging of the real conductivity distribution, so the resolution of the method is weak in both the horizontal and the vertical direction. However, it is a good method for the background conductivity determination, which can be useful for the subsequent application of EM migration.

Another approach is based on the time-domain analogue of the Niblett or Bostic transform (Niblett & Sayn-Wittgenstein 1960), which was developed for magnetotelluric data interpretation. This transform involves algebraic or differential transformations of the apparent resistivity magnetotelluric sounding curve. We can apply the same type of transform to the TDEM apparent resistivity curve, calculated, for example, for the late time field generated by a horizontal loop transmitter on the surface of the earth by the following formula (Spies & Frischknecht 1991):

$$\rho_a(t) = \frac{m^{2/3}\mu_0}{20^{2/3}\pi t^{5/3}}\left(\frac{-\partial H_z}{\partial t}\right)^{-2/3},$$

where $m = nAI$ is the magnetic dipole moment (nA is turns-area, I is the current in the transmitter loop).

The TDEM analogue of the Bostic transform can be developed as follows. In as much as ρ_a is a weighted average resistivity, it might be represented approximately as

$$\rho_a \approx z \Big/ \int_0^z \sigma(z')\,dz', \tag{43}$$

where the running variable z is an *effective depth of penetration*, defined as follows (Nabighian & Macnae 1991):

$$z = \sqrt{2t\rho_a(t)/\mu_0}. \tag{44}$$

Then,

$$z/\rho_a \approx \int_0^z \sigma(z')\,dz'.$$

Differentiating both sides of this last equation with respect to z, we obtain

$$\rho(z) = \left[\frac{d}{dz}\left(\frac{z}{\rho_a}\right)\right]^{-1}, \tag{45}$$

where

$$\frac{d}{dz}\frac{z}{\rho_a} = \frac{1}{\rho_a} - \frac{z}{\rho_a^2}\frac{d\rho_a}{dz} = \frac{1}{\rho_a} - \frac{d\rho_a}{\rho_a}\Big/\frac{dz}{z}. \tag{46}$$

On the strength of eq. (44),

$$\frac{dz}{z} = \left(\frac{d\sqrt{t}}{\sqrt{t}} + \frac{1}{2}\frac{d\rho_a}{\rho_a}\right). \tag{47}$$

Substituting eq. (47) into (46), and then into (45), we finally obtain

$$\rho(z) = \rho_a(2+M)/(2-M),$$

where

$$M = \frac{d\rho_a}{\rho_a}\Big/\frac{d\sqrt{t}}{\sqrt{t}} = d\log\rho_a/d\log\sqrt{t}.$$

The Bostic transformation can be used for determining the background resistivity, σ_b, distribution if we apply this transformation to spatially filtered data.

7.2 Numerical method of EM migration through media with an arbitrary distribution of background conductivity, σ_b

The problem of EM migration through media with an arbitrary distribution of background conductivity, σ_b, can be solved in one of two ways.

(1) The first approach is based on the direct numerical solution of eq. (38) with the boundary conditions (37), using, for example, the finite-difference method. In the paper by Wang *et al.* (1994) there is an example of the application of the finite-difference method for the solution of the same eq. (38) for the back-propagated field. The only difference in our case will be in using different boundary conditions, those given by eq. (37). This is related to the fact that the migrated field in our case is the solution of the boundary-value problem for the observed anomalous (or residual) field in the reverse time.

(2) The second approach is based on application of the integral formulae (40) and (41). It is noteworthy that these equations are the EM counterparts to the Rayleigh integral (Schneider 1978) for seismic wavefields. Calculation of the EM analogue of the Rayleigh integral requires knowledge of the Green's function $G^b(x, z, t|x', z', t')$. In the simplest case of the homogeneous model, $\sigma_b = \text{const.}$, the Green's function is as follows:

$$G^b(x, z, t|x', z', t') = -\frac{1}{4\pi(t-t')}\exp\left\{-\frac{\mu_0\sigma_b}{4(t-t')}[(x'-x)^2 + (z'-z)^2]\right\}. \tag{48}$$

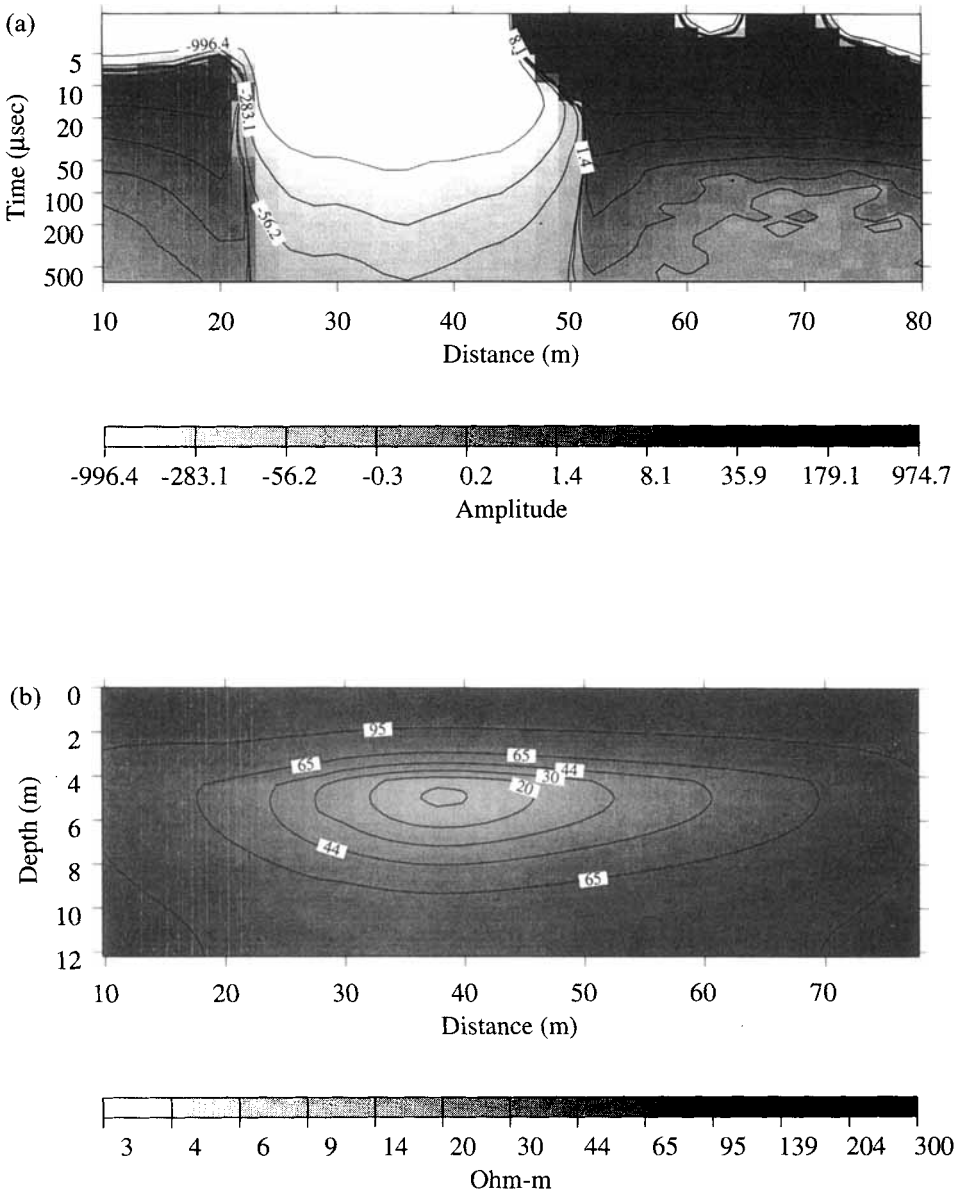

Figure 6. (a) TDEM data observed for the 0 s profile in the Cold Test Pit. (b) Migration apparent resistivity with a homogeneous background for the 0 s profile in the Cold Test Pit.

In the general case of inhomogeneous background conductivity σ_b, the corresponding Green's function can be determined only numerically. However, we can use a simple approach to approximate calculations of the EM analogue of the Rayleigh integral. This approach is based on the approximation of the real inhomogeneous background conductivity by some equivalent effective conductivity, which is different for different points (x', z'), in which we compute the migrated field.

The basic scheme is as follows. On the basis of the Bostic transform or rapid imaging technique, we calculate some approximate model for the background conductivity distribution, which is assumed by definition to be slowly varying in the horizontal direction. The kernel of the EM analogue of the Rayleigh integral is represented by a relatively narrow spatial filter (Zhdanov *et al.* 1988) with its centre at the point $(x', 0)$. We assume that the resistivity varies only in the vertical direction and is described by the function $\rho(x', z)$ within the vertical strip, corresponding to the width of this filter. On a vertical axis, passing through the point $(x', 0)$ for each depth z' we can introduce the effective resistivity, $\rho_{ef}(x', z')$, by a formula similar to (43):

$$\rho_{ef}(x', z') = z' \Big/ \int_0^{z'} \frac{dz}{\rho(x', z)}.$$

Now, we use the EM analogue of the Rayleigh integral formula with the Green's function, computed using eq. (48) with $\sigma_b = 1/\rho_{ef}(x', z')$, for the migration at the point (x', z'). This approximate approach makes it possible to develop fast and simple methods of integral migration through variable background conductivity. We will illustrate the practical effectiveness of this approach in the next section.

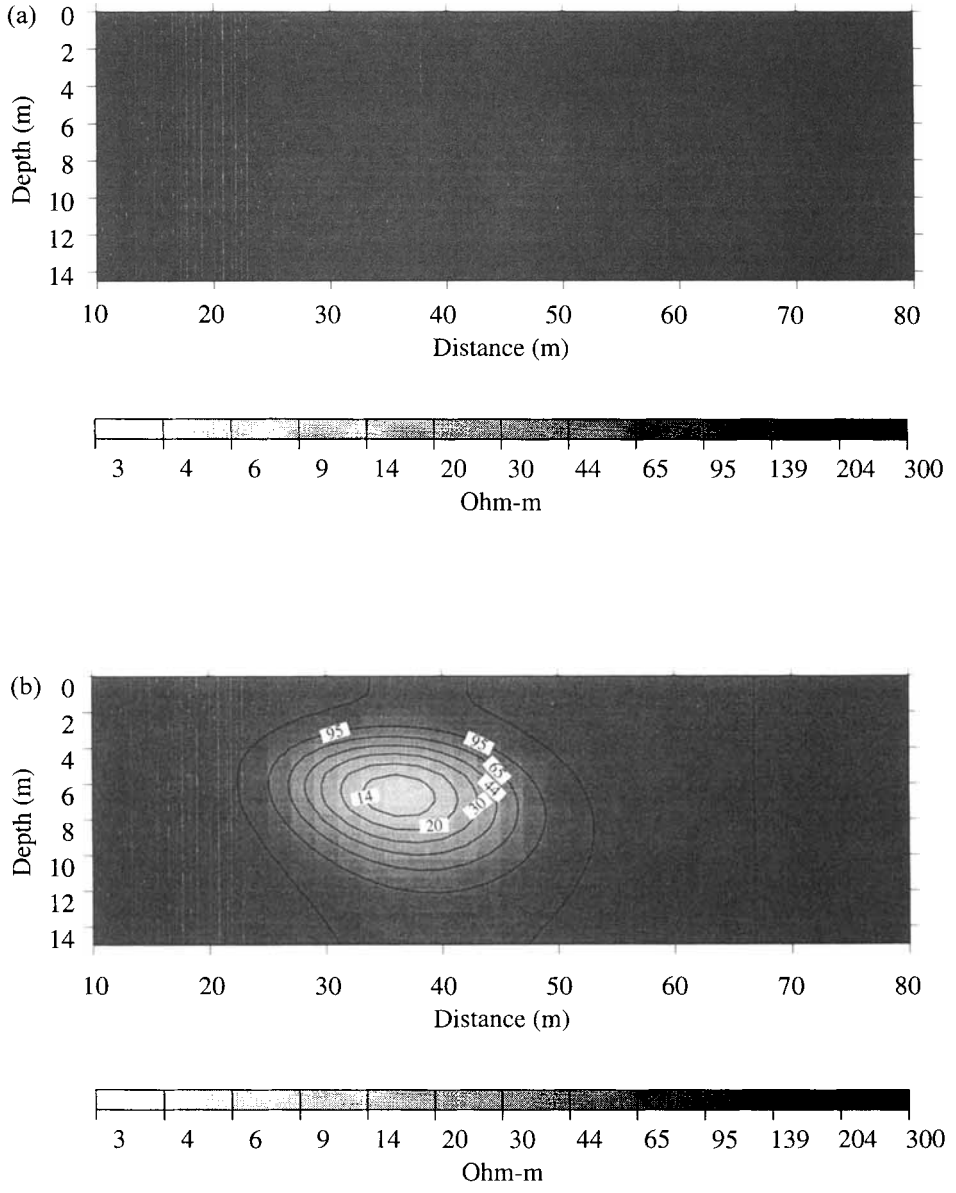

Figure 7. (a) Background apparent resistivity for the 0 s profile in the Cold Test Pit. (b) Migration apparent resistivity with a variable background for the 0 s profile in the Cold Test Pit.

7.3 Approximate imaging conditions

Note that expression (27) involves the calculation of the migrated and incident fields for all moments of time t', which requires expensive computations. In the paper by Zhdanov *et al.* (1995), a simplified approach to migration imaging was developed, based on the calculation of the apparent migration resistivity, $\rho_{ma}(x, z)$, determined for a simple quasi-layered geoelectrical model:

$$\rho_{ma}(x, z) = \left\{\frac{[1+\beta_a^m(x, z)]}{[1-\beta_a^m(x, z)]}\right\}^2 \rho_b(x, z), \tag{49}$$

where $\rho_b = 1/\sigma_b$, and $\beta_a^m(x, z)$ is the apparent reflectivity function.

This function is determined from the values of the migrated residual field (for details see Zhdanov *et al.* 1995).

We emphasize that the migration apparent resistivity, ρ_{ma} is a function of depth. Thus, we obtain the depth geoelectrical cross-section. Actually, the formula (49) can be treated as the approximate solution of the integral equation (27), describing the relations between the migrated anomalous conductivity, $\sigma_{ma}(x', z')$, and the real anomalous conductivity $\sigma_a(x', z')$.

8 TIME-DOMAIN MIGRATION IN THE SOLUTION OF SYNTHETIC EM PROBLEMS

We will illustrate the effectiveness of our method of EM migration and imaging in the solution of inverse problems using some synthetic EM examples. First, we will consider 2-D examples.

8.1 2-D models

The resistivity imaging technique has been tested on the results of numerical modelling with the use of a 2-D finite-difference

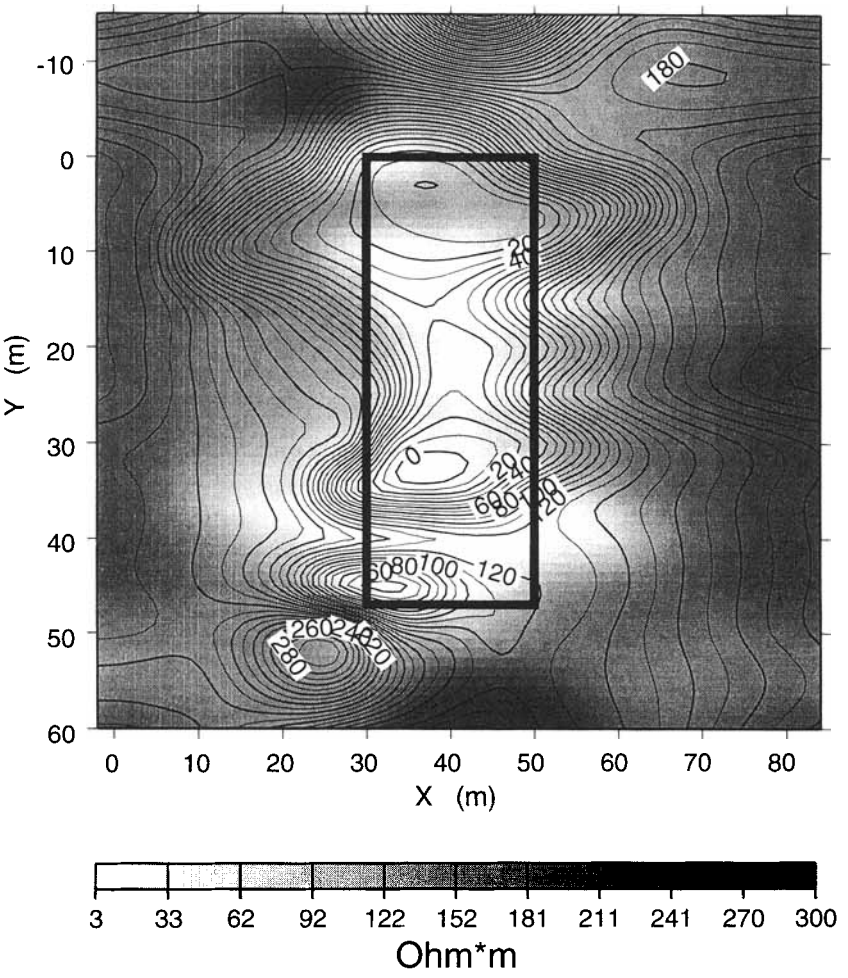

Figure 8. Horizontal migration apparent resistivity map at a depth of 6 m constructed by horizontal interpolation of migration imaging results between the profiles in the Cold Test Pit.

time-domain code (Oristaglio & Hohmann 1984). Fig. 1(a) shows the geoelectrical cross-section of the model, which contains a highly conducting inclusion (on the right) and a poorly conducting inclusion (on the left). The cross-section has a two-layered background conductivity. The EM field in the model was generated by an infinitely long cable. The observed field dH_z/dt was recorded in the time interval from 1 μs to 1000 μs on a logarithmic timescale, with 10 points per decade. The theoretical survey was conducted in the transmitter offset mode, with a transmitter–receiver separation (offset) equal to 4 m. The results of TDEM migration of the secondary field, dH_z/dt, were then recalculated in the migration electric field. This field has been used to compute the migration apparent resistivity in the time domain (Fig. 1b).

The other 2-D model consists of an inhomogeneous near-surface layer with known conductivity and a homogeneous basement, which also contains highly conducting and poorly conducting inclusions (Fig. 2a). The observed field, dH_z/dt, was recorded in the time interval from 1 μs to 1000 μs on a logarithmic timescale, with 10 points per decade. The theoretical survey was also conducted in the transmitter offset mode, with a transmitter–receiver separation (offset) equal to 4 m. The results of the migration through the inhomogeneous background section are shown in Fig. 2(b). One can see very clearly the conductive and resistive bodies on this image.

8.2 3-D model

The next model was of a 3-D conductive body in a homogeneous medium (Fig. 3b). The synthetic data were calculated using a 3-D finite-difference time-domain code (Wang & Hohmann 1993). The EM field in this model was excited by a rectangular loop transmitter (32 m × 32 m), located at a distance of 100 m outside the centre of the rectangular 3-D conducting body. The magnetic induction data ($\partial H_z/\partial t$) were simulated along the profile, passing above the centre of the conductive body (Fig. 3a). It was recorded in the time interval 1 μs–1000 μs on a logarithmic timescale, with 10 points per decade.

For the migration of these data we have used a modified formula (41) with the substitution of the 2-D Green's function by the corresponding 3-D Green's function. This modification makes it possible to migrate the 3-D EM field observed along the profile within the 3-D medium. Actually, this formula can also be obtained from the general 3-D migration formula (12) if we substitute for the surface integral in (12) the curvilinear integral along the profile of observation. From the point of view of the solution of the inverse problem it means that we minimize the residual-field energy flow through the observation profile.

The results of migration imaging, based on the approximate

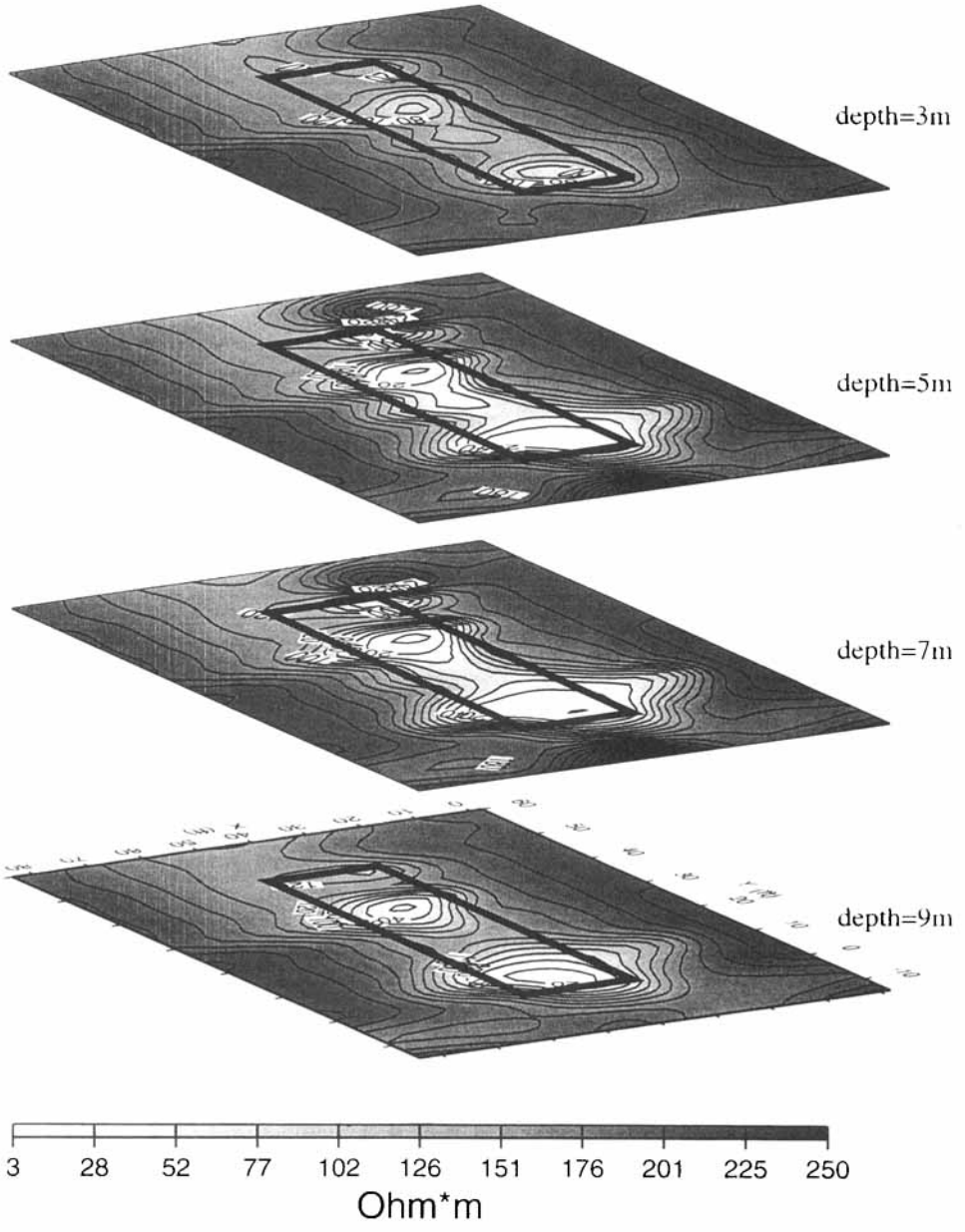

Figure 9. The final 3-D resistivity model of the Cold Test Pit based on rapid imaging and time-domain EM migration.

formula (49), are presented in Fig. 4(a). We have used the migration-imaging conditions (27), based on the convolution between the migrated residual field and the background (incident) field, to produce the image presented in Fig. 4(b).

We can clearly see the conductive body on both of these images. However, the image based on convolution (Fig. 4b) estimates the depth of the conducting body top slightly better than the image in Fig. 4(a), while the shape of the body's vertical cross-section is slightly distorted, possibly by the effect of the primary field. We can also see a resistive shadow to the right of the body. This shadow is the side effect induced by the primary field. We expect that the application of the second or third iteration within the framework of iterative migration could correct this image. Nevertheless, the theoretical advantage of the imaging conditions (27) seems to be that these conditions were derived for an arbitrary geoelectrical model, while conditions (49) were obtained for a simplified quasi-layered model. A further model study should outline the limits of practical applications of all of these imaging conditions.

9 CASE HISTORY: INTERPRETATION OF RWMC TDEM DATA

The time-domain EM migration method has been applied in order to characterize waste sites using time-domain electromagnetic (TDEM) data. The main task was the interpretation of the TDEM data set acquired at the Cold Test Pit site within the Radioactive Waste Management Complex (RWMC) at the Idaho National Engineering Laboratory (INEL) (McLean 1993). The Cold Test Pit was specially designed to test different geophysical methods. The internal structure of the pit was known *a priori* and the results of migration could be checked. A schematic plan of the Pit is presented in Fig. 5. We have processed, by the time-domain electromagnetic migration

method, data obtained as a result of a high-density TDEM profiling survey using a Geonics EM47 instrument along a set of profiles, crossing INEL RWMC Cold Test Pit from the west to the east. The survey was conducted in the transmitter offset or slingram mode, as described by McLean (1993). The transmitter–receiver separation (the distance between the centre of the transmitter loop and the centre of the receiver loop) was equal to 12.5 m. The geoelectrical structure of the pit is 3-D making it impossible to use conventional methods to interpret these data.

In an earlier paper (Zhdanov *et al.* 1995) we used as an effective background resistivity $\rho_b = 100\,\Omega$ m. As a result of processing TDEM data using the migration method we have obtained a set of vertical cross-sections of the Cold Test Pit for a homogeneous background cross-section. The observed TDEM data and the typical cross-sections of the migration apparent resistivity along the profile 0 S (zero South) are presented in Fig. 6.

In this paper we apply a two-step imaging technique to process the same data. On the first step we use rapid imaging, developed by Eaton & Hohmann (1989), to produce a background conductivity distribution, which is presented in Fig. 7(a). On the second step we use the migration through this variable background to compute the resistivity image of the vertical cross-section (Fig. 7b). As we can see, the new migration image is close to the old one (Fig. 6b), but has a variable background resistivity distribution. Fig. 8 shows the horizontal resistivity map at a depth of 6 m obtained by horizontal interpolation of migration-imaging results between the profiles. The final 3-D resistivity model of the Cold Test Pit (Fig. 9), based on rapid imaging and time-domain EM migration, consists of several horizontal resistivity maps for different depths. It demonstrates that this method can be used to determine the structure of anomalous resistivity distribution in INEL RWMC Cold Test Pit. The migration image compares well with the schematic model of the pit that has been provided by the constructors (Fig. 5). The depths and the locations of the conductive sections of the pit also correspond well with the known structure of the pit.

10 CONCLUSIONS

In this paper we have described new results in the development of the electromagnetic migration method. First, we demonstrated that EM migration can be viewed as the solution of the inverse EM problem, formulated as the minimization of the residual EM-field energy flow through the surface of observations. Second, we generalized the EM migration method and theory for 3-D geoelectrical structures and 3-D EM data. Third, we developed a method of EM field migration through a variable-background geoelectrical cross-section. We have tested the method on 2-D and 3-D geoelectrical models, typical for mining and oil and gas exploration.

These new results permit the application of the EM migration method to the interpretation of real TDEM data, collected in 3-D geoelectrical structures. We have illustrated the practical results of time-domain EM migration by applying it to the actual TDEM field data collected at the Cold Test Pit site within the Radioactive Waste Management Complex at the Idaho National Engineering Laboratory.

ACKNOWLEDGMENTS

The authors acknowledge the support of the University of Utah Consortium of Electromagnetic Modeling and Inversion (CEMI), which includes Advanced Power Technologies, BHP, INCO, Japan National Oil Company, Mindeco, MIM Exploration, Naval Research Laboratory, Newmont Exploration, RTZ-Kennecott-CRA, Shell International Exploration and Production, Schlumberger-Doll Research, Western Atlas, Western Mining, Unocal Geothermal Corporation and Zonge Engineering.

We would also like to thank David McLean for providing TDEM data at the Cold Test Pit, and Peter Traynin for his help with using the RIT method and constructing a 3-D image of the Cold Test Pit.

REFERENCES

Barnett, C.T., 1984. Simple inversion of time-domain electromagnetic data, *Geophysics,* **49,** 925–933.

Claerbout, J.F., 1985. Imaging the Earth Interior, *Blackwell Scientific,* Oxford.

Eaton, P.A. & Hohmann, G.W., 1989. A rapid inversion technique for transient electromagnetic soundings, *PEPI,* **53,** 384–404.

Felsen, L.B. & Marcuvitz, N., 1973. Radiation and Scattering of Waves, *Prentice-Hall, Englewood Cliffs, NJ.*

Fletcher, R., 1987. Practical Methods of Optimization, Wiley & Sons, New York, NY.

Macnae, J. & Lamontagne, Y., 1987. Imaging quasi-layered conductive structures by simple processing of transient electromagnetic data, *Geophysics,* **52,** 545–554.

McLean, H.D., 1993. *Time domain electromagnetic survey of three waste burial pits at INEL Radioactive Waste Management Complex,* TTP AL 911201-G2, Chem-Nuclear Geotech, Inc.

Morse, P.M. & Feshbach, H., 1953. Methods of Theoretical Physics, *McGraw-Hill,* New York, NY.

Nabighian, M.N., 1979. Quasi-static transient response of a conducting half-space—an approximate representation, *Geophysics,* **44,** 1700–1705.

Nabighian, M.N. & Macnae, J.C., 1991. Time domain electromagnetic prospecting method, *Electromagnetic Methods in appl. Geophys.,* **2,** Part A, SEG, 427–475.

Niblett, E.R. & Sayn-Wittgenstein, C., 1960. Variation of electrical conductivity with depth by the magnetotelluric method, *Geophysics,* **25,** 948–1008.

Oristaglio, M. & Hohmann, G., 1984. Diffusion of electromagnetic fields into a two-dimensional Earth: A finite-difference approach, *Geophysics,* **49,** 870–894.

Pankratov, O.V., Avdeev, D.B. & Kuvshinov, A.V., 1995. Scattering of electromagnetic field in inhomogeneous earth. Forward problem solution, *Fizika Zemli,* **3,** 17–25.

Schneider, W.A., 1978. Integral formulation for migration in two and three dimensions, *Geophysics,* **43,** 49–76.

Spies, B.R. & Frischknecht, F.C., 1991. Electromagnetic sounding, *Electromagnetic methods in appl. Geophys.,* **2,** Part A, SEG, 285–378.

Stratton, J.A., 1941. Electromagnetic theory, *McGraw-Hill,* New York, NY.

Tarantola A., 1987. *Inverse Problem Theory,* Springer-Verlag, Berlin.

Tikhonov, A.N. & Arsenin, V.Y., 1977. *Solution of Ill-poised Problems,* Winston and Sons, New York, NY.

Wang, T. & Hohman, G.W., 1993. A finite-difference time domain solution for three-dimensional electromagnetic modeling, *Geophysics,* **58,** 797–809.

Wang, T., Oristaglio, M., Tripp, A. & Hohmann, G., 1994. Inversion of diffusive electromagnetic data by a conjugate-gradient method, *Radio Sci.,* **9,** 1143–1156.

Zhdanov, M.S., 1988. Integral Transforms in Geophysics, Springer, Berlin.

Zhdanov, M.S. & Keller, G.V., 1994. *The Geoelectrical Methods in Geophysical Exploration*, Elsevier, Amsterdam.

Zhdanov, M.S., Matusevich, V.U. & Frenkel, M.A., 1988. *Seismic and Electromagnetic Migration,* Nauka, Moscow (in Russian).

Zhdanov, M.S., Traynin, P. & Portniaguine, O., 1995. Resistivity imaging by time domain electromagnetic migration (TDEMM), *Expl. Geophys.*, **26,** 186–194.

Zhdanov, M.S., Traynin, P. & Booker, J.R., 1996. Underground imaging by frequency domain electromagnetic migration, *Geophysics,* **61,** 666–682.

APPENDIX A: ELECTROMAGNETIC GREEN'S TENSORS

The electromagnetic Green's tensors, $\hat{G}_E^b$, $\hat{G}_H^b$, being fields of an elementary electric source, follow Maxwell's equations (Felsen & Marcuvitz 1973):

$$\begin{aligned}\nabla\times\hat{G}_H^b&=\sigma_b\hat{G}_E^b+\hat{i}\delta(\mathbf{r}-\mathbf{r}')\delta(t-t'),\\ \nabla\times\hat{G}_E^b&=-\mu\frac{\beta\hat{G}_H^b}{\partial t};\end{aligned}\tag{A1}$$

they are causal:

$$\hat{G}_E^b(\mathbf{r},t|\mathbf{r}',t')\equiv 0,\qquad \hat{G}_H^b(\mathbf{r},t|\mathbf{r}',t')\equiv 0,\qquad t\le t'.$$

Eq. (A1) suggests that $\hat{G}_E^b$ also satisfies the equation

$$\nabla\times\nabla\times\hat{G}_E^b=-\mu\sigma_b\frac{\partial\hat{G}_E^b}{\partial t}-\mu\hat{i}\delta(\mathbf{r}-\mathbf{r}')\frac{\partial\delta(t-t')}{\partial t}.\tag{A2}$$

The EM Green's tensors exhibit symmetry and can be shown, using the Lorentz lemma, to satisfy the following reciprocal relations (Stratton 1941):

$$\begin{aligned}\hat{G}_E^b(\mathbf{r},t|\mathbf{r}',t')&=\widetilde{\hat{G}}_E^b(\mathbf{r}',-t'|\mathbf{r},-t),\\ \hat{G}_H^b(\mathbf{r},t|\mathbf{r}',t')&=\widetilde{\hat{G}}_H^b(\mathbf{r}',-t'|\mathbf{r},-t),\end{aligned}\tag{A3}$$

where the large tilde denotes the operation of transposition.

The last conditions show that by replacing the source and receiver (that is the points $\mathbf{r}'$ and $\mathbf{r}$) and by going simultaneously to the reverse time, $-t$ (therefore, by retaining the causality, because the condition $t<t'$ in ordinary time implies the condition $-t>-t'$ in reverse time), we obtain the equivalent EM field, described by the Green's tensors $\hat{G}_E^b(\mathbf{r}',t'|\mathbf{r},t)$ and $\hat{G}_H^b(\mathbf{r}',t'|\mathbf{r},t)$.

Following Morse & Feshbach (1953) and Felsen & Marcuvitz (1973) we can introduce also the adjoint Green's tensors:

$$\begin{aligned}\hat{G}_E^{b+}(\mathbf{r},t|\mathbf{r}',t')&=\widetilde{\hat{G}}_E^b(\mathbf{r}',t'|\mathbf{r},t),\\ \hat{G}_H^{b+}(\mathbf{r},t|\mathbf{r}',t')&=\widetilde{\hat{G}}_H^b(\mathbf{r}',t'|\mathbf{r},t).\end{aligned}\tag{A4}$$

They satisfy the following equations, obtained from (A1) by reversing the sign of all space–time coordinates:

$$\begin{aligned}\nabla\times\hat{G}_H^{b+}&=-\sigma_b\hat{G}_E^{b+}-\hat{i}\delta(\mathbf{r}-\mathbf{r}')\delta(t-t'),\\ \nabla\times\hat{G}_E^{b+}&=-\mu\frac{\partial\hat{G}_H^{b+}}{\partial t},\end{aligned}\tag{A5}$$

and eq. (A2) takes the form

$$\nabla\times\nabla\times\hat{G}_E^{b+}=\mu\sigma_b\frac{\partial\hat{G}_E^{b+}}{\partial t}+\mu\hat{i}\delta(\mathbf{r}-\mathbf{r}')\frac{\partial\delta(t-t')}{\partial t}.\tag{A6}$$

The adjoint Green's tensors are anticasual:

$$\hat{G}_E^{b+}(\mathbf{r},t|\mathbf{r}',t')\equiv 0,$$

$$\hat{G}_H^{b+}(\mathbf{r},t|\mathbf{r}',t')\equiv 0,\qquad t\ge t'.$$

APPENDIX B: TENSOR STATEMENTS OF THE GAUSS AND GREEN FORMULAE

This appendix briefly describes the fundamental theorems of tensor analysis, which are widely used in our paper. The notation closely follows the monograph of Zhdanov (1988), where one can find further details.

Let $\hat{G}=\hat{G}(\mathbf{r})$ be a tensor field differentiable continuously everywhere in the domain D right to its boundary S. The tensor statement of the Gauss theorem can be expressed by the following formula:

$$\iiint_D\nabla\cdot\hat{G}dv=\iint_S\mathbf{n}\cdot\hat{G}ds,\tag{B1}$$

where $\mathbf{n}$ is the unit vector of an outward-pointing normal to S.

The Green tensor formula derives from the expression (B1). Indeed, let us specify an auxiliary tensor field $\hat{G}(\mathbf{r})$:

$$\hat{G}=\mathbf{F}\times[\nabla\times\hat{P}]+[\nabla\times\mathbf{F}]\times\hat{P},$$

where $\mathbf{F}$ and $\hat{P}$ are arbitrary vector and tensor fields, respectively, twice continuously differentiable in the domain D (up to its boundary S). The algebraic calculations show that

$$\nabla\cdot\hat{G}=[\nabla\times\nabla\times\mathbf{F}]\cdot\hat{P}-\mathbf{F}\cdot[\nabla\times\nabla\times\hat{P}].\tag{B2}$$

Substituting eq. (B2) into the Gauss tensor formula (B1) we write in the final form the Green tensor formula

$$\begin{aligned}&\iiint_D\{[\nabla\times\nabla\times\mathbf{F}]\cdot\hat{P}-\mathbf{F}\cdot[\nabla\times\nabla\times\hat{P}]\}\,dv\\ &=\iint_S\mathbf{n}\cdot\{\mathbf{F}\times[\nabla\times\hat{P}]+[\nabla\times\mathbf{F}]\times\hat{P}\}\,ds.\end{aligned}\tag{B3}$$

If the vector field $\mathbf{F}$ is replaced by the tensor field $\hat{Q}$, we arrive at another Green tensor formula:

$$\begin{aligned}&\iiint_D\{[\nabla\times\nabla\times\hat{Q}]\cdot\hat{P}-\hat{Q}\cdot[\nabla\times\nabla\times\hat{P}]\}\,dv\\ &=\iint_S\mathbf{n}\cdot\{\hat{Q}\times[\nabla\times\hat{P}]+[\nabla\times\hat{Q}]\times\hat{P}\}\,ds.\end{aligned}\tag{B4}$$

Finally, if the tensor field $\hat{P}$ in eq. (B3) is replaced by the vector field $\mathbf{B}$, we obtain the Green vector formula

$$\begin{aligned}&\iiint_D\{[\nabla\times\nabla\times\mathbf{F}]\cdot\mathbf{B}-[\nabla\times\nabla\times\mathbf{B}]\cdot\mathbf{F}\}\,dv\\ &=\iint_S\mathbf{n}\cdot\{\mathbf{F}\times[\nabla\times\mathbf{B}]-\mathbf{B}\times[\nabla\times\mathbf{F}]\}\,ds.\end{aligned}\tag{B5}$$

APPENDIX C: DETERMINATION OF THE OPTIMAL STEP k_0

Let us determine the optimal step length k_0. To do so we can substitute eq. (24) into (4), in which the integral operator is linearized, using the Born approximation, and calculate the approximate electric field for the model with anomalous

conductivity, $\sigma_{a(1)}(\mathbf{r})$:

$$\mathbf{E}^{(1)}_{pr}(\mathbf{r}, t) \approx \mathbf{E}^{b}(\mathbf{r}, t) + \int_{-\infty}^{\infty} \iiint_{D} \hat{G}^{b}_{E}(\mathbf{r}, t|\mathbf{r}', t') \cdot \sigma_{a(1)}(\mathbf{r}) \mathbf{E}^{b}(\mathbf{r}', t')\, dv'\, dt', \tag{C1}$$

$$\mathbf{H}^{(1)}_{pr}(\mathbf{r}, t) \approx \mathbf{H}^{b}(\mathbf{r}, t) + \int_{-\infty}^{\infty} \iiint_{D} \hat{G}^{b}_{E}(\mathbf{r}, t|\mathbf{r}', t') \cdot \sigma_{a(1)}(\mathbf{r}) \mathbf{E}^{b}(\mathbf{r}', t')\, dv'\, dt'. \tag{C2}$$

Thus, we have the following for the residual-field energy flow functional:

$$\Phi(\sigma_{a(1)}) = \Phi[\sigma_{b}(x, z) - k_0 l_0(x, z)] = \Phi(k_0) = \int_{-\infty}^{\infty} \iint_{S} [\mathbf{E}^{\Delta(1)}(\mathbf{r}, t) \times \mathbf{H}^{\Delta(1)}(\mathbf{r}, t)] \cdot \mathbf{n}\, ds\, dt, \tag{C3}$$

where

$$\mathbf{E}^{\Delta(1)}(\mathbf{r}, t) = \mathbf{E}_{obs}(\mathbf{r}, t) - \mathbf{E}^{(1)}_{pr}(\mathbf{r}, t), \qquad \mathbf{H}^{\Delta(1)}(\mathbf{r}, t) = \mathbf{H}_{obs}(\mathbf{r}, t) - \mathbf{H}^{(1)}_{pr}(\mathbf{r}, t). \tag{C4}$$

Substituting eqs (C4), (C1) and (C2) into (C3), and taking into account eq. (24), we obtain

$$\begin{aligned}\Phi(\sigma_{a(1)}) &= \Phi[\sigma_{b}(x, z) - k_0 l_0(x, z)] \\ &= \int_{-\infty}^{\infty} \iint_{S} [\mathbf{E}_{obs}(\mathbf{r}, t) - \mathbf{E}^{(1)}_{pr}(\mathbf{r}, t)] \times [\mathbf{H}_{obs}(\mathbf{r}, t) - \mathbf{H}^{(1)}_{pr}(\mathbf{r}, t)] \cdot \mathbf{n}\, ds\, dt \\ &\approx \int_{-\infty}^{\infty} \iint_{S} [\mathbf{E}^{\Delta}(\mathbf{r}, t) + k_0 \mathbf{E}^{l_0}(\mathbf{r}', t')] \times [\mathbf{H}^{\Delta}(\mathbf{r}, t) + k_0 \mathbf{H}^{l_0}(\mathbf{r}', t')] \cdot \mathbf{n}\, ds'\, dt',\end{aligned}$$

where the field $\{\mathbf{E}^{l_0}, \mathbf{H}^{l_0}\}$ is an electromagnetic field, calculated using the Born approximation for the geoelectrical model, perturbed in the gradient direction:

$$\mathbf{E}^{l_0}(\mathbf{r}, t) = \int_{-\infty}^{\infty} \iiint_{D} \hat{G}^{b}_{E}(\mathbf{r}, t|\mathbf{r}', \mathbf{t}') \cdot l_0(\mathbf{r}') \mathbf{E}^{b}(\mathbf{r}', \mathbf{t}')\, dv'\, dt',$$

$$\mathbf{H}^{l_0}(\mathbf{r}, t) = \int_{-\infty}^{\infty} \iiint_{D} \hat{G}^{b}_{H}(\mathbf{r}, t|\mathbf{r}', \mathbf{t}') \cdot l_0(\mathbf{r}') \mathbf{E}^{b}(\mathbf{r}', \mathbf{t}')\, dv'\, dt'.$$

Now we can find the first variation of $\Phi(k_0)$ with respect to k_0:

$$\delta\Phi(k_0) = \delta k_0 \int_{-\infty}^{\infty} \iint_{S} \{[\mathbf{E}^{\Delta}(\mathbf{r}, t) + k_0 \mathbf{E}^{l_0}(\mathbf{r}', t')] \times \mathbf{H}^{l_0}(\mathbf{r}', t') - [\mathbf{H}^{\Delta}(\mathbf{r}, t) + k_0 \mathbf{H}^{l_0}(\mathbf{r}', t')] \times \mathbf{E}^{l_0}(\mathbf{r}', t')\} \cdot \mathbf{n}\, ds'\, dt' = 0.$$

The necessary condition for the minimum of $\Phi(k_0)$ is

$$\delta\Phi(k_0) = 0.$$

From the last equation we have

$$k_0 = \frac{1}{2}\left\{\int_{-\infty}^{\infty} \iint_{S} [\mathbf{H}^{l_0}(\mathbf{r}', t') \times \mathbf{E}^{\Delta}(\mathbf{r}, t) + \mathbf{H}^{\Delta}(\mathbf{r}, t) \times \mathbf{E}^{l_0}(\mathbf{r}', t')] \cdot \mathbf{n}\, ds'\, dt'\right\} \cdot \left\{\int_{-\infty}^{\infty} \iint_{S} \mathbf{E}^{l_0}(\mathbf{r}', t') \times \mathbf{H}^{l_0}(\mathbf{r}', t') \cdot \mathbf{n}\, ds'\, dt'\right\}^{-1}. \tag{C5}$$